
Semi-Parametric Deep Neural Networks in Linear Time and Memory

Richa Rastogi^{1*}, Yuntian Deng², Ian Lee³

Mert R. Sabuncu⁴, Volodymyr Kuleshov¹

¹ Department of Computer Science, Cornell University

² Department of Computer Science, Harvard University

³ Department of Computational Biology, Cornell University

⁴ Department of Electrical and Computer Engineering, Cornell University

Abstract

Recent advances in deep learning have been driven by large-scale parametric models, which can be computationally expensive and lack interpretability. Semi-parametric methods query the training set at inference time and can be more compact, although they typically have quadratic computational complexity. Here, we introduce SPIN, a general-purpose semi-parametric neural architecture whose computational cost is linear in the size and dimensionality of the data. Our architecture is inspired by inducing point methods and relies on a novel application of cross-attention between datapoints. At inference time, its computational cost is constant in the training set size as the data gets distilled into a fixed number of inducing points. We find that our method reduces the computational requirements of existing semi-parametric models by up to an order of magnitude across a range of datasets and improves state-of-the-art performance on an important practical problem, genotype imputation.

1 Introduction

Recent advances in deep learning have been driven by large-scale *parametric* models [45, 19, 9, 56, 53]. Modern parametric models rely on large numbers of weights to capture the signal contained in the training set and to facilitate generalization [22, 39]; as a result, they require non-trivial computational resources [35], have limited interpretability [5], and impose a significant carbon footprint [7].

This paper focuses on an alternative *semi-parametric* approach, in which we have access to the training set $\mathcal{D}_{\text{train}} = \{\mathbf{x}^{(i)}, \mathbf{y}^{(i)}\}_{i=1}^n$ at inference time and learn a parametric mapping $\mathbf{y} = f_{\theta}(\mathbf{x} \mid \mathcal{D}_{\text{train}})$ conditioned on this dataset. Semi-parametric models can *query the training set* $\mathcal{D}_{\text{train}}$ and can therefore express rich and interpretable mappings with a compact f_{θ} . Examples of the semi-parametric framework in deep learning include retrieval-augmented language models [54, 31, 28], and non-parametric transformers [43, 66]. However, existing approaches are often specialized to specific tasks (e.g., language modeling [54, 31, 28] or sequence generation [29]), and their computation scales superlinearly in the size of the training set [43].

Here, we develop domain-agnostic semi-parametric methods that are effective across a wide range of application areas and that are computationally efficient. Specifically, we introduce semi-parametric inducing point networks (SPIN), a general-purpose architecture whose computational complexity

*Correspondence to rr568@cornell.edu

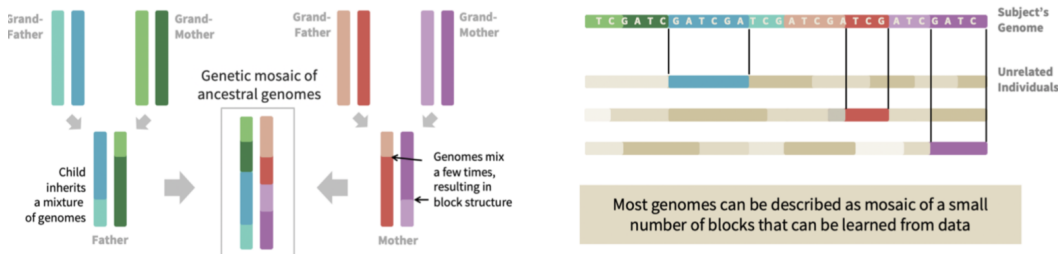


Figure 1: Genotype imputation is a natural candidate for semi-parametric approaches due to the biological principle of recombination.

scales *linearly* in the size of the training set $\mathcal{D}_{\text{train}}$ and the dimensionality of \mathbf{x} . Our architecture is inspired by inducing point approximations for kernel methods [46, 63] and relies on a novel application of attention called *cross-attention between datapoints* [43]. Our approach also learns a *compact encoding* $\mathcal{H}_{\text{train}}$ that replaces $\mathcal{D}_{\text{train}}$ at inference time in downstream applications, resulting in a computational complexity that is constant in $\mathcal{D}_{\text{train}}$ at inference time.

We evaluate our method on a wide range of standard supervised learning benchmarks as well as a motivating real-world application in computational genomics—genotype imputation [48]. We find that our method yields performance improvements, while reducing computation and memory requirements by up to an order of magnitude. In the genomics setting, our approach outperforms one of the highly engineered state-of-the-art software packages - Beagle, widely used within commercial genomics pipelines [11], indicating that our technique has the potential to impact real-world systems.

Contributions In summary, we introduce a semi-parametric neural architecture inspired by inducing point methods whose key component is a novel cross-attention mechanism between data and inducing points. It’s the first general-purpose semi-parametric architecture with the following characteristics:

1. Linear time and space complexity in the size and the dimension of the data during training.
2. The ability to learn a compact encoding of the training set for downstream applications. As a result, at inference time, computational complexity does not depend on training set size.

2 Background

Parametric and Semi-Parametric Machine Learning Most supervised methods in deep learning are *parametric*. Formally, given a training set $\mathcal{D}_{\text{train}} = \{\mathbf{x}^{(i)}, \mathbf{y}^{(i)}\}_{i=1}^n$ with features $\mathbf{x} \in \mathcal{X}$ and labels $\mathbf{y} \in \mathcal{Y}$, we seek to learn the parameters $\theta \in \Theta$ of a mapping $\mathbf{y} = f_{\theta}(\mathbf{x})$ using supervised learning. Crucially, the learning signal from $\mathcal{D}_{\text{train}}$ is fully contained in the parameters θ , whose dimension stays *fixed*.

In contrast, non-parametric approaches learn a mapping $\mathbf{y} = f_{\theta}(\mathbf{x} \mid \mathcal{D}_{\text{train}})$ that can query the training set $\mathcal{D}_{\text{train}}$ at inference time; when the mapping f_{θ} has parameters, the approach is called *semi-parametric*. Many deep learning algorithms—including memory-augmented architectures [29, 59], retrieval-based language models [54, 31, 28], and non-parametric transformers [43]—are instances of this approach. Semi-parametric approaches are often specialized to specific tasks, and their computation scales superlinearly in the size of the training set [43]. This paper develops domain-agnostic semi-parametric methods that are computationally efficient.

A Motivating Application: Genotype Imputation A specific motivating example for developing efficient semi-parametric methods is the problem of genotype imputation (Figure 1). Consider the problem of determining the genomic sequence $\mathbf{y} \in \{A, T, C, G\}^k$ of an individual; rather than directly measuring \mathbf{y} , it is common to use an inexpensive microarray device to measure a small subset of genomic positions $\mathbf{x} \in \{A, T, C, G\}^p$, where $p \ll k$. Genotype imputation is

the task of determining \mathbf{y} from \mathbf{x} via statistical methods and a dataset $\mathcal{D}_{\text{train}} = \{\mathbf{x}^{(i)}, \mathbf{y}^{(i)}\}_{i=1}^n$ of fully-sequenced individuals [48].

Imputation is part of most standard genome analysis workflows. It is also a natural candidate for semi-parametric approaches [47]: a query genome \mathbf{y} can normally be represented as a combination of sequences $\mathbf{y}^{(i)}$ from $\mathcal{D}_{\text{train}}$ because of the biological principle of recombination [41], as shown in Figure 1. Additionally, the problem is a poor fit for parametric models: k can be as high as 10^9 and there is little correlation across non-proximal parts of \mathbf{y} . Thus, we need an unwieldy number of parametric models (one per a subset of \mathbf{y}), whereas a single semi-parametric model can run imputation across the genome.

Attention Mechanisms Our approach for designing semi-parametric models relies on modern attention mechanisms [60], specifically *dot-product attention* $\text{Att}(\mathbf{Q}, \mathbf{K}, \mathbf{V})$, which combines a query matrix $\mathbf{Q} \in \mathbb{R}^{d_q \times e_q}$ with key and value matrices $\mathbf{K} \in \mathbb{R}^{d_v \times e_q}$, $\mathbf{V} \in \mathbb{R}^{d_v \times e_v}$ as

$$\text{Att}(\mathbf{Q}, \mathbf{K}, \mathbf{V}) = \text{softmax}(\mathbf{Q}\mathbf{K}^T / \sqrt{e_q})\mathbf{V}.$$

To attend to different aspects of the keys and values, multi-head attention (MHA) extends this mechanism via e_h attention heads:

$$\text{MHA}(\mathbf{Q}, \mathbf{K}, \mathbf{V}) = \text{concat}(\mathbf{O}_1, \dots, \mathbf{O}_{e_h})\mathbf{W}^O \quad \mathbf{O}_j = \text{Att}(\mathbf{Q}\mathbf{W}_j^Q, \mathbf{K}\mathbf{W}_j^K, \mathbf{V}\mathbf{W}_j^V)$$

Each attention head projects $\mathbf{Q}, \mathbf{K}, \mathbf{V}$ into a lower-dimensional space using learnable projection matrices $\mathbf{W}_j^Q, \mathbf{W}_j^K \in \mathbb{R}^{e_q \times e_{qh}}$, $\mathbf{W}_j^V \in \mathbb{R}^{e_v \times e_{vh}}$ and mixes the outputs of the heads using $\mathbf{W}^O \in \mathbb{R}^{e_h e_{vh} \times e_o}$. As is commonly done, we assume that $e_{vh} = e_v / e_h$, $e_{qh} = e_q / e_h$, and $e_o = e_q$.

Given two matrices $\mathbf{X}, \mathbf{H} \in \mathbb{R}^{d \times e}$, a multi-head attention block (MAB) wraps MHA together with layer normalization and a fully connected layer²:

$$\text{MAB}(\mathbf{X}, \mathbf{H}) = \mathbf{O} + \text{FF}(\text{LayerNorm}(\mathbf{O})) \quad \mathbf{O} = \mathbf{X} + \text{MHA}(\text{LayerNorm}(\mathbf{X}), \mathbf{H}, \mathbf{H})$$

Previous applications of multi-head attention to semi-parametric models [43] scale quadratically in the dataset size; our work is inspired by efficient attention architectures [38, 46] and develops scalable semi-parametric models with linear computational complexity.

3 Method

3.1 A Framework for Semi-Parametric Learning Based on Neural Inducing Points

A key challenge posed by semi-parametric methods—one affecting both classical kernel methods [32] as well as recent attention-based approaches [43]—is the $O(n^2)$ computational cost per gradient update at training time, due to pairwise comparisons between training set points³. Our work introduces methods that reduce this cost to $O(hn)$ —where $h \ll n$ is a hyper-parameter—without sacrificing performance.

Neural Inducing Points Our approach is based on *inducing points*, a technique popular in approximate kernel methods [46, 63]. A set of inducing points $\mathcal{H} = \{\mathbf{h}^{(j)}\}_{j=1}^h$ can be thought of as a “virtual” set of training instances that can replace the training set $\mathcal{D}_{\text{train}}$. Intuitively, when $\mathcal{D}_{\text{train}}$ is large, many datapoints are redundant—for example, groups of similar $\mathbf{x}^{(i)}$ can be replaced with a single inducing point $\mathbf{h}^{(j)}$ with little loss of information.

The key challenge in developing inducing point methods is finding a good set \mathcal{H} . While classical approaches rely on optimization techniques [63], we use an *attention mechanism* to produce \mathcal{H} . Each inducing point $\mathbf{h}^{(j)} \in \mathcal{H}$ attends over the training set $\mathcal{D}_{\text{train}}$ to select its relevant “neighbors” and updates itself based on them. We implement attention between \mathcal{H} and $\mathcal{D}_{\text{train}}$ in $O(hn)$ time.

²We use the pre-norm parameterization for residual connections and omit details such as dropout, see Nguyen and Salazar [52] for the full parameterization.

³By default we use gradient descent instead of stochastic gradient descent, which has the benefit that a query point gets to attend to all the training points rather than a subset only. In Section 4.4, we will introduce a batching setting where each gradient update is approximated using a subset of the training set.

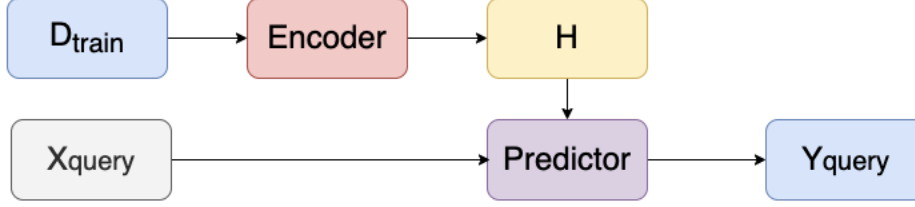


Figure 2: High-level model structure. An encoder compresses the training data $\mathcal{D}_{\text{train}}$ into inducing points \mathbf{H} , and then a predictor makes predictions based on test input $\mathbf{X}_{\text{query}}$ while querying the inducing points \mathbf{H} .

Dataset Encoding Note that once we have a good set of inducing points \mathcal{H} , it becomes possible to discard $\mathcal{D}_{\text{train}}$ and use \mathcal{H} instead for all future predictions. The parametric part of the model makes predictions based on \mathcal{H} only. This feature is an important capability of our architecture; computational complexity is now independent of \mathcal{D} and we envision this feature being useful in applications where sharing $\mathcal{D}_{\text{train}}$ is not possible (e.g., for computational or privacy reasons).

3.2 Semi-Parametric Inducing Point Networks

Next, we describe semi-parametric inducing point networks (SPIN), a domain-agnostic architecture with linear-time complexity.

Notation and Data Embedding The SPIN model relies on a training set $\mathcal{D}_{\text{train}} = \{\mathbf{x}^{(i)}, \mathbf{y}^{(i)}\}_{i=1}^n$ with a sequence of input features $\mathbf{x}^{(i)} \in \mathcal{X} \subseteq \mathcal{V}_x^p$ and a sequence of labels $\mathbf{y}^{(i)} \in \mathcal{Y} \subseteq \mathcal{V}_y^k$ where \mathcal{V}_x and \mathcal{V}_y are input and output vocabulary respectively⁴; we embed each dimension (each attribute) of \mathbf{x} and \mathbf{y} into an e -dimensional embedding and represent $\mathcal{D}_{\text{train}}$ as a tensor of embeddings $\mathbf{D} \in \mathbb{R}^{n \times d \times e}$, where $d = p + k$ is obtained from concatenating the sequence of embeddings for each $\mathbf{x}^{(i)}$ and $\mathbf{y}^{(i)}$. The set $\mathcal{D}_{\text{train}}$ is used to learn inducing points $\mathcal{H} = \{\mathbf{h}^{(j)}\}_{j=1}^h$; similarly, we represent \mathcal{H} via a tensor $\mathbf{H} \in \mathbb{R}^{h \times f \times e}$ of $h \leq n$ inducing points, each being a sequence of $f \leq d$ embeddings of size e .

To make predictions and measure loss on a set of b examples $\mathcal{D}_{\text{query}} = \{\mathbf{x}^{(i)}, \mathbf{y}^{(i)}\}_{i=1}^b$, we use the same embedding procedure to obtain a tensor of input embeddings $\mathbf{X}_{\text{query}} \in \mathbb{R}^{b \times d \times e}$ by embedding $\{\mathbf{x}^{(i)}, \mathbf{0}\}_{i=1}^b$, in which the labels have been masked with zeros. We also use a tensor $\mathbf{Y}_{\text{gold}} \in \mathbb{R}^{b \times d}$ to store the ground truth labels and inputs (the objective function we use requires the model to make predictions on masked input elements as well, see below for details).

High-Level Model Structure Figure 2 presents an overview of SPIN modules. At a high level, there are two components: (1) an Encoder module, which takes as input $\mathcal{D}_{\text{train}}$ and returns a tensor of inducing points \mathbf{H} ; and (2) a Predictor module, which is a fully parametric model that outputs logits $\mathbf{Y}_{\text{query}}$ from \mathbf{H} and $\mathbf{X}_{\text{query}}$.

$$\mathbf{H} = \text{Encoder}(\mathcal{D}_{\text{train}}) \quad \mathbf{Y}_{\text{query}} = \text{Predictor}(\mathbf{X}_{\text{query}}, \mathbf{H})$$

The encoder consists of a sequence of layers, each of which takes as input $\mathbf{D} \in \mathbb{R}^{n \times d \times e}$ and two tensors $\mathbf{H}_A \in \mathbb{R}^{n \times f \times e}$ and $\mathbf{H}_D \in \mathbb{R}^{h \times f \times e}$ and output updated versions of \mathbf{H}_A , \mathbf{H}_D for the next layer. Each layer consists of a sequence of up to three cross-attention layers described below. The final output \mathbf{H} of the encoder is the \mathbf{H}_D produced by the last layer.

3.2.1 Encoder Architecture

Each layer of the encoder consists of three sublayers denoted as XABA, XABD, ABLA:

$$\mathbf{H}'_A = \text{XABA}(\mathbf{H}_A, \mathbf{D}) \quad \mathbf{H}'_D = \text{XABD}(\mathbf{H}_D, \mathbf{H}'_A) \quad \mathbf{H}_A = \text{ABLA}(\mathbf{H}'_A) \quad \mathbf{H}_D = \text{ABLA}(\mathbf{H}'_D)$$

⁴Here we consider the case where both input and output are discrete, but our approach is easily generalizable to continuous input and output spaces.

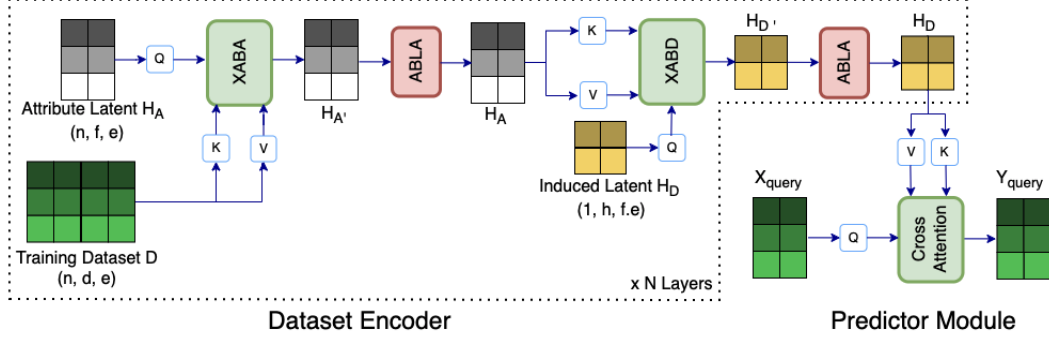


Figure 3: SPIN Architecture. Each layer of the encoder consists of sublayers XABA, ABLA, XABD, and ABLA, and the predictor consists of a cross attention layer. We omit feedforward layers for simplicity.

Cross-Attention Between Attributes (XABA) An XABA layer captures the dependencies among attributes via cross-attention between the sequence of latent encodings in \mathbf{H} and the sequence of datapoint features in \mathbf{D} .

$$\text{XABA}(\mathbf{H}_A, \mathbf{D}) = \text{MAB}(\mathbf{H}_A, \mathbf{D})$$

This updates the features of each datapoint in \mathbf{H}_A to be a combination of the features of the corresponding datapoints in \mathbf{D} . In effect, this reduces the dimensionality of the datapoints (from $n \times d \times e$ to $n \times f \times e$). The time complexity of this layer is $O(ndfe)$, where f is the dimensionality of the reduced tensor.

Cross-Attention Between Datapoints (XABD) The XABD layer is the key module that takes into account the entire training set to generate inducing points. First, it reshapes (“unfolds”) its input tensors $\mathbf{H}'_A \in \mathbb{R}^{n \times f \times e}$ and $\mathbf{H}_D \in \mathbb{R}^{h \times f \times e}$ into ones of dimensions $(1 \times n \times fe)$ and $(1 \times h \times fe)$ respectively. It then performs cross-attention between the two unfolded tensors. The output of cross-attention has dimension $(1 \times h \times fe)$; it is reshaped (“folded”) into an output tensor of size $(h \times f \times e)$.

$$\text{XABD}(\mathbf{H}_D, \mathbf{H}'_A) = \text{fold}(\text{MAB}(\text{unfold}(\mathbf{H}_D), \text{unfold}(\mathbf{H}'_A)))$$

This layer produces inducing points. Each inducing point in \mathbf{H}_D attends to dimensionality-reduced datapoints in \mathbf{H}'_A and uses its selected datapoints to update its own representation. The computational complexity of this operation is $O(nhfe)$, which is linear in training set size n .

Self-Attention Between Latent Attributes (ABLA) The third type of layer further captures dependencies among attributes by computing regular self-attention across attributes:

$$\text{ABLA}(\mathbf{H}'_A) = \text{MAB}(\mathbf{H}'_A, \mathbf{H}'_A) \quad \text{ABLA}(\mathbf{H}'_D) = \text{MAB}(\mathbf{H}'_D, \mathbf{H}'_D)$$

This enables the inducing points to refine their internal representations.

The dataset encoder consists of a sequence of the above layers Figure 3. The ABLA layers are optional based on validation performance. The input \mathbf{H}_D to the first layer is part of the learned model parameters; the initial \mathbf{H}_A is a linear projection of \mathbf{D} . The output of the encoder is the output \mathbf{H}_D of the final layer.

3.2.2 Predictor Architecture

The predictor is a parametric model that maps an input tensor $\mathbf{X}_{\text{query}}$ to an output tensor of logits $\mathbf{Y}_{\text{query}}$. The predictor can use any parametric model; we propose an architecture based on a simple cross-attention operation followed by a linear projection to the vocabulary size as shown in Figure 3:

$$\text{Predict}(\mathbf{X}_{\text{query}}, \mathbf{H}) = \text{FF}(\text{MAB}(\mathbf{X}_{\text{query}}, \mathbf{H}_D))$$

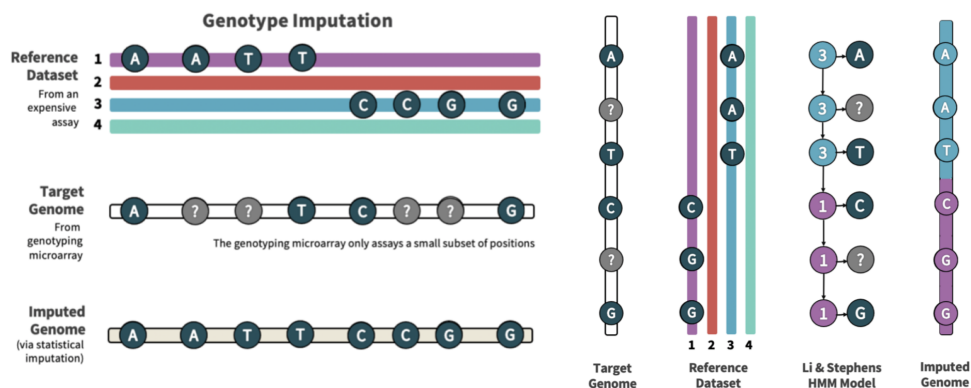


Figure 4: Left: Overview of genotype imputation on a target genome using a reference dataset. Right: Existing non-parametric method for genomic imputation [47].

3.3 Objective Function

To train the model, we use maximum likelihood estimation and maximize the log probability of generating the label part of \mathbf{Y}_{gold} under the predicted logits $\mathbf{Y}_{\text{query}}$. Denote this loss term as $\mathcal{L}^{\text{labels}}$. In addition, following prior works [19, 26, 43], we randomly mask out a subset of input attributes in $\mathbf{X}_{\text{query}}$ and ask the model to reconstruct these masked attributes and denote this loss term $\mathcal{L}^{\text{attributes}}$. The overall training loss is a weighted combination of the loss over label predictions and over the predictions of the masked attributes.

$$\mathcal{L}^{\text{SPIN}} = (1 - \lambda)\mathcal{L}^{\text{labels}} + \lambda\mathcal{L}^{\text{attributes}}$$

Following previous work NPT [43], we start with a weight λ of 0.5 and anneal it to lean towards the loss for predicting labels.

4 Experiments

4.1 Genotype Imputation Experiments

Genotype imputation (Figure 4, left) is the task of inferring the sequence \mathbf{y} of an entire genome via statistical methods from a small subset of positions \mathbf{x} —usually obtained from an inexpensive DNA microarray device [48]—and a dataset $\mathcal{D}_{\text{train}} = \{\mathbf{x}^{(i)}, \mathbf{y}^{(i)}\}_{i=1}^n$ of fully-sequenced individuals [48]. Imputation is part of most standard workflows in genomics [49] and involves mature imputation software (Figure 4, right) [58, 10] that benefits from over a decade of engineering [47]. These systems are fully non-parametric and match genomes in $\mathcal{D}_{\text{train}}$ to \mathbf{x}, \mathbf{y} ; their scalability to modern datasets of up to millions of individuals is a known problem in the field [50]. Improved imputation holds the potential to reduce sequencing costs and improve workflows in medicine and agriculture.

Experiment Setup We compare against one of the state-of-the-art packages, Beagle [10] on the 1000 Genomes dataset [14] following the methodology described in [58]. We use 5008 complete sequences \mathbf{y} that we divide into train/val/test split of 0.86, 0.12, and 0.02 respectively. We construct inputs \mathbf{x} by masking positions that do not appear on the Illumina Omni2.5 array [67]. Our experiments focus on five sections of the genome for chromosome 20 and we pre-process the input into sequences of K -mers for all methods (see Appendix A.1). The performance of this task is measured with Pearson correlation coefficient R^2 between the imputed SNP and the actual value of SNP at a particular position.

We additionally compare against NPTs, Set Transformers, and classical machine learning methods. NPT-16, SPIN-16 and Set Transformer-16 refer to embedding dimension 16, model depth 4, attention head 1, while NPT-64, SPIN-64 and Set Transformer-64 refer to embedding dimension 64, model depth 4, and attention heads 4. SPIN uses 10 inducing points for datapoints and for each attribute

($h=10, f=10$). A batch size of 256 is used for Transformer methods and we train using the lookahead Lamb optimizer [71].

Table 1: Performance Summary on Genomic Sequence Imputation. A difference of 0.5% is statistically significant at pvalue 0.05.

Approach		Parametric	Pearson $R^2 \uparrow$	Param Count \downarrow	Complexity
Traditional ML	Gradient Boosting	True	87.63	-	-
	MLP	True	95.31	65M	-
	KNN	False	89.70	-	-
Bio Software	Beagle	False	95.64	-	$O(n^2)$
Transformer	NPT-16	False	95.87	16.7M	$O(n^2)$
	Set Transformer-16	False	95.90	33.4M	$O(hn)$
	SPIN-16	False	96.04	8.1M	$O(hn)$

Results Table 1 presents the main results for genotype imputation. Compared to the previous state-of-the-art commercial software Beagle, which is specialized in this task, all Transformer-based methods achieve strong performance, despite making fewer assumptions and being more general. Among the Transformer-based approaches, SPIN achieves the highest Pearson R^2 , at a fraction of other methods’ number of parameters. Among traditional ML approaches, MLP performs the best. However, all the traditional ML methods are trained using one model per output position (per component of \mathbf{y}); the hyper-parameters of each model are also tuned separately. As a result, this process is not scalable and requires a very high number of parameters. We provide memory requirements (Peak GPU Memory usage in GB), average train time per epoch, and details on hyper-parameter tuning in Appendix A.1.

4.2 UCI Experiments

We present experimental results for 6 standard UCI benchmarks, namely Yacht, Concrete, Boston-Housing (regression datasets), Kick, Income, and Breast Cancer (classification datasets). We evaluate SPIN with relevant transformer baselines such as NPT [44] and a baseline we developed by incorporating inducing set point blocks (ISAB) introduced by Set Transformer [46] as a drop-in replacement for the multi-head attention blocks used in NPT. We also evaluate against Gradient Boosting [23], MLP [34, 27], KNN [2]. Following Kossen et al. [43] we measure the average ranking of methods and standard deviation based on these tasks. To show the memory efficiency of our approach we also report the Peak GPU Memory usage and standard deviation as a fraction of GPU Mem used by NPT for different splits of the test dataset in Table 2.

Table 2: Performance Summary on UCI Datasets.

Approach		Average Ranking order \downarrow	Peak GPU Mem (relative to NPT) \downarrow
Traditional ML	Gradient Boosting	3.00 ± 2.00	-
	MLP	3.83 ± 1.94	-
	KNN	5.33 ± 1.21	-
Transformer	NPT	2.83 ± 1.47	1.0x
	Set Transformer	3.00 ± 1.22	$1.67 \pm 0.51x$
	SPIN	2.83 ± 1.33	$0.52 \pm 0.21x$

Results SPIN and NPT achieve the best average ranking order on UCI datasets, but SPIN uses half the GPU memory compared to NPT. We provide detailed results on each of the datasets and hyperparameter details in Appendix A.2. Additionally, SPIN uses one-third of the parameters at inference time, for instance on the Yacht dataset, NPT has 42.7M parameters during training and inference, SPIN has 33.1M parameters during training but the SPIN modules used at inference have only 10.0M parameters since we can directly use learned latent instead of the training data.

4.3 Ablation Analysis

To evaluate the effectiveness of each module we introduced, we perform ablation analysis by gradually removing components from SPIN. Both SPIN-16 and SPIN-64 consist of 2 layers each of XABA, XABD, and ABLA for a model depth of 4. We remove components one at a time and compare the performance with default modules. In Table 3 we observe that for both SPIN-64 and SPIN-16, XABD (cross-attention between datapoints) is a crucial component, and incorporating ABLA (self-attention between latents) can sometimes help as in the case of SPIN-16.

Table 3: Ablation Analysis on Genomics Dataset (SNPs 424600-424700)

Model	Approach	Pearson R^2 \uparrow
SPIN-64	SPIN (XABA+XABD+ABLA)	94.01
	- XABD	93.33
	- ABLA	94.24
	- XABA - ABLA	94.07
SPIN-16	SPIN (XABA+XABD+ABLA)	94.26
	- XABD	88.47
	- ABLA	94.09
	- XABA - ABLA	94.31

4.4 Effect of Batching

One way to alleviate the memory and computational burden of scaling non-parametric Transformers to large datasets is batching, where the train/val/test datasets are split into multiple slices, and gradients are only estimated on one slice at a time [43]. While batching allows for scaling to large datasets, the training time per epoch increases as the batch size goes down. In Appendix A.3. we show that on the UCI dataset Kick, while NPT with batching gets a comparable classification accuracy, our approach SPIN uses 5x less GPU memory, 3x fewer parameters, and 2x less average training time per epoch. On the genomics dataset, Table 4 shows the comparison between different batching regimes for both NPT and SPIN. We observe that SPIN consumes half the memory and training time per epoch. The computational efficiency of SPIN is orthogonal to the strategy of batching.

Table 4: Effect of Batching on Genomics Dataset (SNPs 287600-287700).

Approach	Batch Size	Pearson R^2 \uparrow	Peak GPU Mem (GB)	Avg. Train time/epoch(s) \downarrow
NPT	No Batching	96.84	18.21	1.03
	2048	96.74	10.49	1.34
	1024	96.83	9.24	1.73
	256	96.85	8.12	4.39
SPIN	No Batching	97.06	6.08	0.52
	2048	97.01	3.86	0.86
	1024	97.04	3.44	1.22
	256	97.07	2.97	3.64

4.5 Compute Resources

For all the experiments, we use one 24GB NVIDIA GeForce RTX 3090 GPU. We do not use multi-GPU training or other memory-saving techniques such as gradient checkpointing, pruning, mixed precision training, etc. but note that these are orthogonal to our approach and can be used to further reduce the computational complexity.

5 Related Work

Non-Parametric and Semi-Parametric Methods Non-parametric methods have a long history in machine learning, starting from nearest neighbors approaches [21, 3] and density estimation [24], and including more recent approaches based on kernels [17], such as Gaussian processes [57] and support vector machines [32]. Kernel methods are a classical example of non-parametric approaches with quadratic complexity [4], which motivates a long line of approximate methods based on random projections [1], Fourier analysis [55], and inducing point methods [64]. Inducing points have been widely applied in kernel machines [51], Gaussian processes classification [36], regression [12], semi-supervised learning [18], and more [33]. Our work combines non-parametric inducing points methods with deep learning and attention.

Deep Semi-Parametric Models Deep Gaussian Processes [16], Deep Kernel Learning [65], and Neural Processes [25] build upon classical methods. Deep GPs rely on sophisticated variational inference methods [62], making them challenging to implement, while Neural Processes and their attentive versions [42] rely on multiple samples of datasets, not unlike in meta-learning [20]. Retrieval augmented transformers [8] use attention to query external datasets in specific domains such as language modeling [28] and question answering [69], and in a way that is similar to earlier memory-augmented models [29]. Non-Parametric Transformers (NPTs) [44] use a domain-agnostic architecture based on attention that runs in $O(n^2 d^2)$ at training time and $O(nd^2)$ at inference time; NPTs are closest to our work. We leverage their idea of attention over data and improve its scalability to $O(nd)$ at training time and $O(d)$ at inference time.

Attention Mechanisms The quadratic cost of self-attention [60] can be reduced using efficient architectures such as sparse attention [6], Set Transformers [46], the Performer [13], the Nystromer [68], Long Ranger [30], Big Bird [70], the Perceiver [38, 37], and others [40, 61]. Our work most closely resembles the Set Transformer [46] and Perceiver [38, 37] mechanisms—we extend these mechanisms to cross-attention between datapoints and use them to attend to datapoints, similarly to Non-Parametric Transformers [44].

6 Limitations

The SPIN model achieves linear complexity via advanced self-attention mechanisms; This also introduces additional hyper-parameters into the model, potentially increasing tuning time. The resulting architecture remains overparametrized even after with small numbers of inducing points h, f and may overfit.

The primary source of expressivity is attention between datapoints, which has a query dimension he . Highly expressive models may learn to ignore the training set and operate in a fully-parametric mode; this failure mode is best avoided via regularization and large datasets. Interestingly, our approach benefits from big data, while classical non-parametric models work best on small datasets due to their computational complexity. Regularization via small h, f , dropout, and feature masking control overfitting; we will explore more compact architectures in future work.

7 Conclusion

In this paper, we introduce a domain-agnostic general-purpose architecture, the semi-parametric inducing point network (SPIN). Unlike previous semi-parametric approaches whose computational cost grows quadratically with the size of the dataset, our approach scales linearly in the size and dimensionality of the data by leveraging a cross attention mechanism between datapoints and induced latents, allowing it to scale to large datasets.

We present empirical results on six UCI datasets and a real-world important task in genomics, genotype imputation, and show that SPIN can achieve competitive, if not better, performance relative to state-of-the-art methods at a fraction of the computational cost. Furthermore, our approach allows the use of a compact encoding of training dataset at inference time, which is potentially useful for privacy-preserving applications or where retrieving from training data at inference is cost-prohibitive.

References

- [1] Dimitris Achlioptas, Frank McSherry, and Bernhard Schölkopf. Sampling techniques for kernel methods. *Advances in neural information processing systems*, 14, 2001.
- [2] N. S. Altman. An introduction to kernel and nearest-neighbor nonparametric regression. *The American Statistician*, 46(3):175–185, 1992. doi: 10.1080/00031305.1992.10475879. URL <https://www.tandfonline.com/doi/abs/10.1080/00031305.1992.10475879>.
- [3] Naomi S Altman. An introduction to kernel and nearest-neighbor nonparametric regression. *The American Statistician*, 46(3):175–185, 1992.
- [4] Francis Bach. Sharp analysis of low-rank kernel matrix approximations. In *Conference on Learning Theory*, pages 185–209. PMLR, 2013.
- [5] Yonatan Belinkov. Probing classifiers: Promises, shortcomings, and advances. *Computational Linguistics*, 48(1):207–219, 2022.
- [6] Iz Beltagy, Matthew E Peters, and Arman Cohan. Longformer: The long-document transformer. *arXiv preprint arXiv:2004.05150*, 2020.
- [7] Emily M Bender, Timnit Gebru, Angelina McMillan-Major, and Shmargaret Shmitchell. On the dangers of stochastic parrots: Can language models be too big? In *Proceedings of the 2021 ACM Conference on Fairness, Accountability, and Transparency*, pages 610–623, 2021.
- [8] Giovanni Bonetta, Rossella Cancelliere, Ding Liu, and Paul Vozila. Retrieval-augmented transformer-xl for close-domain dialog generation. *arXiv preprint arXiv:2105.09235*, 2021.
- [9] Tom Brown, Benjamin Mann, Nick Ryder, Melanie Subbiah, Jared D Kaplan, Prafulla Dhariwal, Arvind Neelakantan, Pranav Shyam, Girish Sastry, Amanda Askell, et al. Language models are few-shot learners. *Advances in neural information processing systems*, 33:1877–1901, 2020.
- [10] Brian L. Browning, Ying Zhou, and Sharon R. Browning. A one-penny imputed genome from next-generation reference panels. *American Journal of Human Genetics*, 2018. doi: 10.1016/j.ajhg.2018.07.015.
- [11] Brian L Browning, Ying Zhou, and Sharon R Browning. A one-penny imputed genome from next-generation reference panels. *The American Journal of Human Genetics*, 103(3):338–348, 2018.
- [12] Yanshuai Cao, Marcus A Brubaker, David J Fleet, and Aaron Hertzmann. Efficient optimization for sparse gaussian process regression. *Advances in Neural Information Processing Systems*, 26, 2013.
- [13] Krzysztof Marcin Choromanski, Valerii Likhoshesterov, David Dohan, Xingyou Song, Andreea Gane, Tamas Sarlos, Peter Hawkins, Jared Quincy Davis, Afroz Mohiuddin, Lukasz Kaiser, et al. Rethinking attention with performers. In *International Conference on Learning Representations*, 2020.
- [14] Laura Clarke, Susan Fairley, Xiangqun Zheng-Bradley, Ian Streeter, Emily Perry, Ernesto Lowy, Anne-Marie Tassé, and Paul Flicek. The international Genome sample resource (IGSR): A worldwide collection of genome variation incorporating the 1000 Genomes Project data. *Nucleic Acids Research*, 45(D1):D854–D859, 09 2016. ISSN 0305-1048. doi: 10.1093/nar/gkw829. URL <https://doi.org/10.1093/nar/gkw829>.
- [15] Phillip E. C. Compeau, Pavel A. Pevzner, and Glenn Tesler. How to apply de bruijn graphs to genome assembly. *Nature Biotechnology*, 2011. doi: 10.1038/nbt.2023.
- [16] Andreas Damianou and Neil D Lawrence. Deep gaussian processes. In *Artificial intelligence and statistics*, pages 207–215. PMLR, 2013.
- [17] Richard A Davis, Keh-Shin Lii, and Dimitris N Politis. Remarks on some nonparametric estimates of a density function. In *Selected Works of Murray Rosenblatt*, pages 95–100. Springer, 2011.

- [18] Olivier Delalleau, Yoshua Bengio, and Nicolas Le Roux. Efficient non-parametric function induction in semi-supervised learning. In *International Workshop on Artificial Intelligence and Statistics*, pages 96–103. PMLR, 2005.
- [19] Jacob Devlin, Ming-Wei Chang, Kenton Lee, and Kristina Toutanova. BERT: Pre-training of deep bidirectional transformers for language understanding. In *Proceedings of the 2019 Conference of the North American Chapter of the Association for Computational Linguistics: Human Language Technologies, Volume 1 (Long and Short Papers)*, pages 4171–4186, Minneapolis, Minnesota, June 2019. Association for Computational Linguistics. doi: 10.18653/v1/N19-1423. URL <https://aclanthology.org/N19-1423>.
- [20] Chelsea Finn, Pieter Abbeel, and Sergey Levine. Model-agnostic meta-learning for fast adaptation of deep networks. In *International conference on machine learning*, pages 1126–1135. PMLR, 2017.
- [21] Evelyn Fix and Joseph Lawson Hodges. Discriminatory analysis. nonparametric discrimination: Consistency properties. *International Statistical Review/Revue Internationale de Statistique*, 57(3):238–247, 1989.
- [22] Jonathan Frankle and Michael Carbin. The lottery ticket hypothesis: Finding sparse, trainable neural networks. In *International Conference on Learning Representations*, 2018.
- [23] Jerome H. Friedman. Greedy function approximation: A gradient boosting machine. *The Annals of Statistics*, 29(5):1189 – 1232, 2001. doi: 10.1214/aos/1013203451. URL <https://doi.org/10.1214/aos/1013203451>.
- [24] Keinosuke Fukunaga and L Hostetler. Optimization of k nearest neighbor density estimates. *IEEE Transactions on Information Theory*, 19(3):320–326, 1973.
- [25] Marta Garnelo, Jonathan Schwarz, Dan Rosenbaum, Fabio Viola, Danilo J Rezende, SM Eslami, and Yee Whye Teh. Neural processes. *arXiv preprint arXiv:1807.01622*, 2018.
- [26] Marjan Ghazvininejad, Omer Levy, Yinhan Liu, and Luke Zettlemoyer. Mask-predict: Parallel decoding of conditional masked language models. In *Proceedings of the 2019 Conference on Empirical Methods in Natural Language Processing and the 9th International Joint Conference on Natural Language Processing (EMNLP-IJCNLP)*, pages 6112–6121, Hong Kong, China, November 2019. Association for Computational Linguistics. doi: 10.18653/v1/D19-1633. URL <https://aclanthology.org/D19-1633>.
- [27] Xavier Glorot and Yoshua Bengio. Understanding the difficulty of training deep feedforward neural networks. In Yee Whye Teh and Mike Titterton, editors, *Proceedings of the Thirteenth International Conference on Artificial Intelligence and Statistics*, volume 9 of *Proceedings of Machine Learning Research*, pages 249–256, Chia Laguna Resort, Sardinia, Italy, 13–15 May 2010. PMLR. URL <https://proceedings.mlr.press/v9/glorot10a.html>.
- [28] Edouard Grave, Armand Joulin, and Nicolas Usunier. Improving neural language models with a continuous cache. *arXiv preprint arXiv:1612.04426*, 2016.
- [29] Alex Graves, Greg Wayne, and Ivo Danihelka. Neural turing machines. *arXiv preprint arXiv:1410.5401*, 2014.
- [30] Jake Grigsby, Zhe Wang, and Yanjun Qi. Long-range transformers for dynamic spatiotemporal forecasting. *arXiv preprint arXiv:2109.12218*, 2021.
- [31] Kelvin Guu, Kenton Lee, Zora Tung, Panupong Pasupat, and Ming-Wei Chang. Realm: Retrieval-augmented language model pre-training. *arXiv preprint arXiv:2002.08909*, 2020.
- [32] Marti A. Hearst, Susan T Dumais, Edgar Osuna, John Platt, and Bernhard Scholkopf. Support vector machines. *IEEE Intelligent Systems and their applications*, 13(4):18–28, 1998.
- [33] James Hensman, Alexander G Matthews, Maurizio Filippone, and Zoubin Ghahramani. Mcmc for variationally sparse gaussian processes. *Advances in Neural Information Processing Systems*, 28, 2015.

- [34] Geoffrey E. Hinton. Connectionist learning procedures, 1989.
- [35] Jordan Hoffmann, Sebastian Borgeaud, Arthur Mensch, Elena Buchatskaya, Trevor Cai, Eliza Rutherford, Diego de Las Casas, Lisa Anne Hendricks, Johannes Welbl, Aidan Clark, et al. Training compute-optimal large language models. *arXiv preprint arXiv:2203.15556*, 2022.
- [36] Pavel Izmailov and Dmitry Kropotov. Faster variational inducing input gaussian process classification. *arXiv preprint arXiv:1611.06132*, 2016.
- [37] Andrew Jaegle, Sebastian Borgeaud, Jean-Baptiste Alayrac, Carl Doersch, Catalin Ionescu, David Ding, Skanda Koppula, Daniel Zoran, Andrew Brock, Evan Shelhamer, et al. Perceiver io: A general architecture for structured inputs & outputs. *arXiv preprint arXiv:2107.14795*, 2021.
- [38] Andrew Jaegle, Felix Gimeno, Andrew Brock, Andrew Zisserman, Oriol Vinyals, and João Carreira. Perceiver: General perception with iterative attention. *CoRR*, abs/2103.03206, 2021. URL <https://arxiv.org/abs/2103.03206>.
- [39] Jared Kaplan, Sam McCandlish, Tom Henighan, Tom B Brown, Benjamin Chess, Rewon Child, Scott Gray, Alec Radford, Jeffrey Wu, and Dario Amodei. Scaling laws for neural language models. *arXiv preprint arXiv:2001.08361*, 2020.
- [40] Angelos Katharopoulos, Apoorv Vyas, Nikolaos Pappas, and François Fleuret. Transformers are rnns: Fast autoregressive transformers with linear attention. In *International Conference on Machine Learning*, pages 5156–5165. PMLR, 2020.
- [41] John Kendrew. *The Encyclopedia of Molecular Biology*. John Wiley & Sons, 2009.
- [42] Hyunjik Kim, Andriy Mnih, Jonathan Schwarz, Marta Garnelo, Ali Eslami, Dan Rosenbaum, Oriol Vinyals, and Yee Whye Teh. Attentive neural processes. In *International Conference on Learning Representations*, 2018.
- [43] Jannik Kossen, Neil Band, Clare Lyle, Aidan N Gomez, Thomas Rainforth, and Yarin Gal. Self-attention between datapoints: Going beyond individual input-output pairs in deep learning. *Advances in Neural Information Processing Systems*, 34, 2021.
- [44] Jannik Kossen, Neil Band, Clare Lyle, Aidan N. Gomez, Tom Rainforth, and Yarin Gal. Self-attention between datapoints: Going beyond individual input-output pairs in deep learning. *CoRR*, abs/2106.02584, 2021. URL <https://arxiv.org/abs/2106.02584>.
- [45] Alex Krizhevsky, Ilya Sutskever, and Geoffrey E Hinton. Imagenet classification with deep convolutional neural networks. *Advances in neural information processing systems*, 25, 2012.
- [46] Juho Lee, Yoonho Lee, Jungtaek Kim, Adam R. Kosiosek, Seungjin Choi, and Yee Whye Teh. Set transformer. *CoRR*, abs/1810.00825, 2018. URL <http://arxiv.org/abs/1810.00825>.
- [47] Na Li and Matthew Stephens. Modeling linkage disequilibrium and identifying recombination hotspots using single-nucleotide polymorphism data. *Genetics*, 165(4):2213–2233, 2003.
- [48] Yun Li, Cristen Willer, Serena Sanna, and Gonçalo Abecasis. Genotype imputation. *Annual review of genomics and human genetics*, 10:387–406, 2009.
- [49] Runyang Nicolas Lou, Arne Jacobs, Aryn P Wilder, and Nina Overgaard Therkildsen. A beginner’s guide to low-coverage whole genome sequencing for population genomics. *Molecular Ecology*, 30(23):5966–5993, 2021.
- [50] Altti Ilari Maarala, Kalle Pärn, Javier Nuñez-Fontarnau, and Keijo Heljanko. Sparkbeagle: Scalable genotype imputation from distributed whole-genome reference panels in the cloud. In *Proceedings of the 11th ACM International Conference on Bioinformatics, Computational Biology and Health Informatics*, pages 1–8, 2020.
- [51] Timothy Nguyen, Zhouong Chen, and Jaehoon Lee. Dataset meta-learning from kernel ridge-regression. In *International Conference on Learning Representations*, 2020.

- [52] Toan Q. Nguyen and Julian Salazar. Transformers without tears: Improving the normalization of self-attention. In *Proceedings of the 16th International Conference on Spoken Language Translation*, Hong Kong, November 2-3 2019. Association for Computational Linguistics. URL <https://aclanthology.org/2019.iwslt-1.17>.
- [53] Matthew E. Peters, Mark Neumann, Mohit Iyyer, Matt Gardner, Christopher Clark, Kenton Lee, and Luke Zettlemoyer. Deep contextualized word representations. In *Proceedings of the 2018 Conference of the North American Chapter of the Association for Computational Linguistics: Human Language Technologies, Volume 1 (Long Papers)*, pages 2227–2237, New Orleans, Louisiana, June 2018. Association for Computational Linguistics. doi: 10.18653/v1/N18-1202. URL <https://aclanthology.org/N18-1202>.
- [54] Jack W Rae, Sebastian Borgeaud, Trevor Cai, Katie Millican, Jordan Hoffmann, Francis Song, John Aslanides, Sarah Henderson, Roman Ring, Susannah Young, et al. Scaling language models: Methods, analysis & insights from training gopher. *arXiv preprint arXiv:2112.11446*, 2021.
- [55] Ali Rahimi and Benjamin Recht. Random features for large-scale kernel machines. *Advances in neural information processing systems*, 20, 2007.
- [56] Aditya Ramesh, Prafulla Dhariwal, Alex Nichol, Casey Chu, and Mark Chen. Hierarchical text-conditional image generation with clip latents. *arXiv preprint arXiv:2204.06125*, 2022.
- [57] Carl Edward Rasmussen. Gaussian processes in machine learning. In *Summer school on machine learning*, pages 63–71. Springer, 2003.
- [58] Simone Rubinacci, Olivier Delaneau, and Jonathan Marchini. Genotype imputation using the positional burrows wheeler transform. *PLOS Genetics*, 2020. doi: 10.1371/journal.pgen.1009049.
- [59] Adam Santoro, Sergey Bartunov, Matthew Botvinick, Daan Wierstra, and Timothy Lillicrap. Meta-learning with memory-augmented neural networks. In *International conference on machine learning*, pages 1842–1850. PMLR, 2016.
- [60] Ashish Vaswani, Noam Shazeer, Niki Parmar, Jakob Uszkoreit, Llion Jones, Aidan N Gomez, Łukasz Kaiser, and Illia Polosukhin. Attention is all you need. *Advances in neural information processing systems*, 30, 2017.
- [61] Sinong Wang, Belinda Z Li, Madian Khabsa, Han Fang, and Hao Ma. Linformer: Self-attention with linear complexity. *arXiv preprint arXiv:2006.04768*, 2020.
- [62] Yali Wang, Marcus Brubaker, Brahim Chaib-Draa, and Raquel Urtasun. Sequential inference for deep gaussian process. In *Artificial Intelligence and Statistics*, pages 694–703. PMLR, 2016.
- [63] Andrew Wilson and Hannes Nickisch. Kernel interpolation for scalable structured gaussian processes (kiss-gp). In *International conference on machine learning*, pages 1775–1784. PMLR, 2015.
- [64] Andrew Gordon Wilson, Christoph Dann, and Hannes Nickisch. Thoughts on massively scalable gaussian processes. *arXiv preprint arXiv:1511.01870*, 2015.
- [65] Andrew Gordon Wilson, Zhiting Hu, Ruslan Salakhutdinov, and Eric P Xing. Deep kernel learning. In *Artificial intelligence and statistics*, pages 370–378. PMLR, 2016.
- [66] Sam Wiseman and Karl Stratos. Label-agnostic sequence labeling by copying nearest neighbors. In *Proceedings of the 57th Annual Meeting of the Association for Computational Linguistics*, pages 5363–5369, Florence, Italy, July 2019. Association for Computational Linguistics. doi: 10.18653/v1/P19-1533. URL <https://aclanthology.org/P19-1533>.
- [67] Wrayner. Human omni marker panel. URL <https://www.well.ox.ac.uk/~wrayner/strand/>.

- [68] Yunyang Xiong, Zhanpeng Zeng, Rudrasis Chakraborty, Mingxing Tan, Glenn Fung, Yin Li, and Vikas Singh. Nyströmformer: A nystöm-based algorithm for approximating self-attention. In *Proceedings of the... AAAI Conference on Artificial Intelligence. AAAI Conference on Artificial Intelligence*, volume 35, page 14138. NIH Public Access, 2021.
- [69] Zhilin Yang, Peng Qi, Saizheng Zhang, Yoshua Bengio, William Cohen, Ruslan Salakhutdinov, and Christopher D. Manning. HotpotQA: A dataset for diverse, explainable multi-hop question answering. In *Proceedings of the 2018 Conference on Empirical Methods in Natural Language Processing*, pages 2369–2380, Brussels, Belgium, October–November 2018. Association for Computational Linguistics. doi: 10.18653/v1/D18-1259. URL <https://aclanthology.org/D18-1259>.
- [70] Manzil Zaheer, Guru Guruganesh, Kumar Avinava Dubey, Joshua Ainslie, Chris Alberti, Santiago Ontanon, Philip Pham, Anirudh Ravula, Qifan Wang, Li Yang, et al. Big bird: Transformers for longer sequences. *Advances in Neural Information Processing Systems*, 33: 17283–17297, 2020.
- [71] Michael Zhang, James Lucas, Jimmy Ba, and Geoffrey E Hinton. Lookahead optimizer: k steps forward, 1 step back. *Advances in Neural Information Processing Systems*, 32, 2019.

Appendix: Semi-Parametric Deep Neural Networks in Linear Time and Memory

A Experimental Details

A.1 Genomic Sequence Imputation

Imputation is performed on single-nucleotide polymorphisms (SNPs) with a corresponding marker panel specifying the microarray. We randomly sample five sections of the genome for chromosome 20 for conducting experiments. Each section is selected with 100 SNPs to be predicted and 150 closest SNPs are obtained. For compact encoding of SNPs, we form K -mers, which are commonly used in various genomics applications [15], where K is a hyper-parameter that controls the granularity of tokenization (how many nucleotides are treated as a single token). This now becomes a 2^K -way classification task. We set K to 5 for all the genomics experiments, so that there are 20 (100/5) target SNPs to be imputed and 30 (150/5) attributes per sampled section. We report pearson R^2 for each of the five sections in Table 5. For computational load, we report peak GPU memory usage in GB where applicable, an average of train time per epoch in seconds and parameter count per method.

Hyper-parameters for tuning We provide the list of hyper-parameters that were grid searched for different methods in Table 6. Beagle is a specialized software using dynamic programming and does not require any hyper-parameters from the user.

Table 5: Performance on Genomics Imputation

Approach		Pearson $R^2 \uparrow$	Peak GPU Mem (GB) \downarrow	Params Count \downarrow	Avg. Train time/epoch(s) \downarrow
Genomics Dataset (SNPs 68300-68400)					
Traditional ML	Gradient Boosting	81.12	-	-	-
	MLP	97.63	-	-	-
	KNN	86.96	-	-	-
Bio Software	Beagle	98.07	-	-	-
Transformer	NPT	96.91	0.45	16.7M	2.22
	Set Transformer	96.73	0.76	33.4M	2.93
	SPIN	97.21	0.28	8.0M	2.23
Genomics Dataset (SNPs 169500-169600)					
Traditional ML	Gradient Boosting	91.53	-	-	-
	MLP	97.19	-	-	-
	KNN	95.65	-	-	-
Bio Software	Beagle	97.87	-	-	-
Transformer	NPT	97.46	0.45	16.7M	1.98
	Set Transformer	97.39	0.76	33.4M	2.99
	SPIN	97.46	0.28	8.0M	2.76
Genomics Dataset (SNPs 287600-287700)					
Traditional ML	Gradient Boosting	81.12	-	-	-
	MLP	96.20	-	-	-
	KNN	95.56	-	-	-
Bio Software	Beagle	92.62	-	-	-
Transformer	NPT	97.10	0.45	16.7M	2.24
	Set Transformer	97.15	0.76	33.4M	2.99
	SPIN	97.15	0.28	8.0M	2.60
Genomics Dataset (SNPs 424600-424700)					
Traditional ML	Gradient Boosting	82.77	-	-	-
	MLP	91.98	-	-	-
	KNN	84.39	-	-	-
Bio Software	Beagle	93.72	-	-	-
Transformer	NPT	94.12	0.45	16.7M	2.23
	Set Transformer	94.02	0.76	33.4M	2.90
	SPIN	94.26	0.28	8.0M	2.21
Genomics Dataset (SNPs 543000-543100)					
Traditional ML	Gradient Boosting	72.66	-	-	-
	MLP	89.56	-	-	-
	KNN	78.22	-	-	-
Bio Software	Beagle	94.58	-	-	-
Transformer	NPT	89.69	0.45	16.7M	1.95
	Set Transformer	92.12	0.76	33.4M	2.52
	SPIN	91.50	0.28	8.0M	2.28

Table 6: Hyperparameters for Genomics Dataset

Model	Hyperparameter	Setting
NPT, SPIN, Set Transformer	Embedding Dimension	[16, 128]
	Depth	[2, 8]
	Label Masking	[0, 0.5]
	Target Masking	[0.3]
	Learning rate	$[1e - 5, 1e - 2]$
	Dropout	[0.4, 0.6]
	Batch Size	[256, 5008 (No Batching)]
Gradient Boosting	Max Depth	[5, 10]
	n_estimators	[100]
	Learning rate	$[1e - 2]$
MLP	Hidden Layer Sizes	[(500, 500, 500)]
	Batch Size	[128, 256]
	L2 regularization	[0, $1e - 2$]
	Learning rate init	$[1e - 4, 1e - 2]$
KNN	n_neighbors	[2, 1000]
	weights	[distance]
	algorithm	[auto]
	Leaf Size	[10, 100]
Bio Software	None	None

A.2 UCI Regression Tasks

In Table 7, we report performance and computational requirements for 10 cv splits for Yacht dataset, 3 cv splits for Boston Housing and 6 cv splits for Concrete dataset. The lower number of cv splits for Boston-Housing and Concrete are due to computational load requirements for these datasets.

Yacht dataset consists of 308 instances, 5 categorical features and 1 continuous target

Boston Housing dataset consists of 506 instances, 13 continuous features and 1 continuous target

Concrete consists of 1030 instances, 8 continuous features and 1 continuous target

Table 7: Performance on UCI Regression Datasets

Approach		RMSE ↓	Peak GPU Mem (GB) ↓	Params Count ↓	Avg. Train time/epoch(s) ↓
Boston-Housing					
Traditional ML	Gradient Boosting	2.60 ± 0.38	-	-	-
	MLP	2.78 ± 0.28	-	-	-
	KNN	3.79 ± 0.68	-	-	-
Transformer	NPT	2.46 ± 0.27	8.2	168.0M	1.43
	Set Transformer	2.40 ± 0.21	16.5	336.0M	1.62
	SPIN	2.54 ± 0.25	6.2	168.0M	1.43
Yacht					
Traditional ML	Gradient Boosting	0.87 ± 0.37	-	-	-
	MLP	0.83 ± 0.18	-	-	-
	KNN	11.97 ± 2.06	-	-	-
Transformer	NPT	1.42 ± 0.64^5	2.1	42.7M	0.10
	Set Transformer	1.29 ± 0.34	4.1	85.4M	0.19
	SPIN	1.28 ± 0.66	1.6	32.2M	0.07
Concrete					
Traditional ML	Gradient Boosting	4.61 ± 0.72	-	-	-
	MLP	5.29 ± 0.74	-	-	-
	KNN	8.62 ± 0.77	-	-	-
Transformer	NPT	5.43 ± 0.61	3.4	69.9M	0.13
	Set Transformer	5.35 ± 0.80	6.8	139.9M	0.21
	SPIN	5.99 ± 0.33	1.9	38.3M	0.13

A.3 UCI Classification Tasks

In Table 8, we report mean and std dev. for classification accuracy over 10 cv splits for Breast Cancer. We report results for 1 cv split for Kick and Income dataset because of computational load.

Breast Cancer dataset consists of 569 instances, 30 continuous features and 1 categorical target.

Kick dataset consists of 72,983 instances, 14 continuous, 17 categorical features and 1 categorical target.

Income consists of 299,285 instances, 6 continuous, 35 categorical features and 1 categorical target. We provide hyperparameters grid searched for UCI datasets in Table 9. Additionally, we provide average ranking separated by Regression and Classification tasks in Table 10 and Table 11 respectively.

⁵NPT reports a mean of 1.27 on this task that we could not reproduce. However, we emphasize that for UCI experiments, all the model parameters are kept same for all the transformer methods.

Table 8: Performance on UCI Classification Datasets

Approach		Accuracy \uparrow	Peak GPU Mem (GB) \downarrow	Params Count \downarrow	Avg. Train time/epoch(s) \downarrow
Breast Cancer					
Traditional ML	Gradient Boosting	94.03 \pm 2.74	-	-	-
	MLP	94.03 \pm 3.05	-	-	-
	KNN	95.26 \pm 2.48	-	-	-
Transformer	NPT	95.79 \pm 1.22	2.6	51.3M	0.15
	Set Transformer	94.91 \pm 1.53	5.2	102.6M	0.21
	SPIN	95.61 \pm 2.22	0.9	16.7M	0.16
Kick					
Traditional ML	Gradient Boosting	90.20	-	-	-
	MLP	89.96	-	-	-
	KNN	87.71	-	-	-
Transformer	NPT	90.04	14.9	232.6M	56.22
	Set Transformer	90.03	15.0	465.0M	52.35
	SPIN	90.06	3.6	73.7M	27.76
Income					
Traditional ML	Gradient Boosting	95.8	-	-	-
	MLP	95.4	-	-	-
	KNN	94.8	-	-	-
Transformer	NPT	95.6	24	1504M	-
	Set Transformer	-	OOM	OOM	-
	SPIN	95.6	11.5	418.9M	68.02

Table 9: Hyperparameters for UCI Dataset

Model	Hyperparameter	Setting
NPT, SPIN, Set Transformer	Embedding Dimension	[16, 128]
	Depth	[8]
	Label Masking	[0, 0.5]
	Target Masking	[0.3]
	Learning rate	$[1e - 5, 1e - 2]$
	Dropout	[0.4, 0.6]
	Batch Size	[2048, No Batching]
Gradient Boosting	Max Depth	[3, 10]
	n_estimators	[50, 1000]
	Learning rate	$[1e - 3, 0.3]$
MLP (Boston Housing Breast Cancer, Concrete, and Yacht)	Hidden Layer Sizes	$[(25) - (500), (25, 25) - (500, 500), (25, 25, 25) - (500, 500, 500)]$
	Batch Size	[32, 256]
	L2 regularization	[0, 1]
	Learning rate	[constant, invscaling, adaptive]
	Learning rate init	$[1e - 5, 1e - 1]$
MLP (Kick, Income)	Hidden Layer Sizes	$[(25, 25, 25) - (500, 500, 500)]$
	Batch Size	[128, 256]
	L2 regularization	$[0, 1e - 2]$
	Learning rate	[constant, invscaling, adaptive]
	Learning rate init	$[1e - 5, 1e - 1]$
KNN (Boston Housing Breast Cancer, Concrete, and Yacht)	n_neighbors	[2, 100]
	weights	[uniform, distance]
	algorithm	[ball_tree, kd_tree, brute]
	Leaf Size	[10, 100]
KNN (Kick, Income)	n_neighbors	[2, 1000]
	weights	[distance]
	algorithm	[auto]
	Leaf Size	[10, 100]

Table 10: Average Ranking on UCI Regression Dataset (Yacht, Boston Housing, Concrete) based on RMSE

Approach		Average Ranking order \uparrow	Peak GPU Mem (relative to NPT) \downarrow
Traditional ML	Gradient Boosting	2.33 ± 1.53	-
	MLP	2.67 ± 1.53	-
	KNN	6.00 ± 0.00	-
Transformer	NPT	3.67 ± 1.53	1.0x
	Set Transformer	2.67 ± 1.53	$1.99 \pm 0.03x$
	SPIN	3.67 ± 1.15	$0.69 \pm 0.12x$

Table 11: Average Ranking on UCI Classification Dataset (Breast Cancer, Kick, Income based on Classification Accuracy)

Approach		Average Ranking order \uparrow	Peak GPU Mem (relative to NPT) \downarrow
Traditional ML	Gradient Boosting	4.33 ± 1.53	-
	MLP	5.00 ± 1.00	-
	KNN	4.67 ± 1.53	-
Transformer	NPT	2.00 ± 1.00	1.0x
	Set Transformer	3.50 ± 0.70	$1.67 \pm 0.51x$
	SPIN	2.00 ± 1.00	$0.52 \pm 0.21x$